

# Orbital Maneuvering with Electrodynamic Tethers

Steven G. Tragesser\* and Hakan San†

U.S. Air Force Institute of Technology, Wright–Patterson Air Force Base, Ohio 45433

The general perturbation equations are used to develop a guidance algorithm for electrodynamic tethers. The current in the tether is controlled to obtain an arbitrary orbit change for low Earth satellites. The tether is assumed to be perfectly aligned with the local vertical, and tether flexibility is neglected. Several numerical examples are simulated that demonstrate the ability of the guidance to maneuver the vehicle accurately. The guidance scheme is suitable for preliminary assessment of the feasibility and desirability of orbital maneuvering with electrodynamic tethers. The algorithm is also sufficiently robust for potential use onboard an operational vehicle.

## Introduction

ELECTRODYNAMIC tethers can be used as a fuel efficient means to propel spacecraft. Current induced in a conductive tether will interact with the Earth's magnetic field to produce a force that can change the spacecraft's orbit as shown in Fig. 1. This enables orbital maneuvers that use electrical energy without expending propellant. For a hollow cathode plasma contactor (the interface between the current in the tether and the ambient plasma), there is some use of expendable gas to facilitate ion collection and emission, but the mass of this gas is minimal compared to the propellant of more traditional propulsion systems. Furthermore, it may be possible to use field emitter array cathodes, which do not require any expendables.<sup>1,2</sup>

The nearly propellantless nature of maneuvering with electrodynamic tethers could potentially enable new ways of operating in space. Some of these possibilities could be achieved in the near term. For example, techniques for boost and reentry of spacecraft has been developed by several researchers<sup>2–8</sup> and will be demonstrated in the NASA ProSEDS mission. Other applications are also being considered and could reap tremendous benefit. For example, a satellite servicing vehicle could rendezvous with multiple satellites in different orbits to transfer fuel or replace components to extend the lifetime of expensive space assets. An orbital tug could change the orbits of low-Earth-orbit (LEO) satellites.<sup>9</sup> A space surveillance satellite could obtain intelligence on foreign space assets and even perform counterspace missions if necessary.

There are two practical disadvantages to electrodynamic tethers. The first is that the ionosphere density is not sufficient for maneuvering out beyond LEO. Second, for practical currents, for example, a few amperes, the achievable thrust is low, and maneuvers can take many weeks to realize. Therefore, it is necessary to make an electrodynamic tether as autonomous as possible. When human support is limited for these long-duration operations, the electrodynamic tether concept can be made more cost effective.

This paper provides the guidance equations for the tether current to effect a desired change in orbital elements. The guidance is capable of simultaneously changing the orbit size, shape, and plane, that is, semimajor axis, eccentricity, inclination, line of nodes, and argument of perigee. These guidance laws could be used in a mission planner to perform trade studies and to evaluate the performance of a given electrodynamic tether design. The guidance laws may be suitable for onboard implementation as well,

although they do not necessarily yield the minimum time orbit transfer.

## Perturbation Equations

The general perturbation equations governing the evolution of the orbital elements are very useful for determining the form of the guidance law. The force on the spacecraft due to the interaction of the current in the tether,  $I$ , and the Earth's magnetic field  $B$  is<sup>10</sup>

$$F = LI \times B \quad (1)$$

where  $L$  is the length of the tether. The tether is assumed to remain perfectly aligned with the local vertical. In actual operation, electrodynamic forces normal to the tether and orbit–attitude coupling due to nonvanishing eccentricity will cause oscillations away from the local vertical. These oscillations (and the current modulation necessary to control them) will tend to decrease the performance of the tether. Therefore, the results in this paper are ideal. However, one promising study indicates that introducing tether damping via a “dashpot” can reduce in-plane and out-of-plane librations without significantly decreasing the electrodynamic tether performance.<sup>11</sup> For the vertical tether, the vector for the current is

$$I = I(\mathbf{r}/r) = I\hat{e}_r \quad (2)$$

where  $\mathbf{r}$  is the position vector to the spacecraft from the center of the Earth, so that a positive current is away from the Earth. The magnetic field is assumed to be a tilted dipole, with the middle of the Earth as its center<sup>10</sup>:

$$B = (\mu_m/r^3)[\hat{e}_m - 3(\hat{e}_m \cdot \hat{e}_r)\hat{e}_r] \quad (3)$$

where  $\mu_m$  is the magnetic moment of the Earth's dipole ( $8 \times 10^6 \text{ T} \cdot \text{km}^3$ ) and  $\hat{e}_m$  is the axis of the dipole. The dipole is assumed to be fixed in inertial space. This is equivalent to neglecting the tilt of the dipole, which will again yield ideal results. A better magnetic field model should be used for more refined trade studies or an actual onboard system.

For convenience, a modified orbital element set is used, where inclination  $i$  and the argument of the ascending node,  $\Omega$ , are measured with respect to the magnetic equatorial plane instead of the geographic equatorial plane. Then the axis of the magnetic dipole can be expressed in the orbital frame as

$$\hat{e}_m = -\sin(\omega + \nu) \sin i \hat{e}_r - \cos(\omega + \nu) \sin i \hat{e}_\theta - \cos i \hat{e}_w \quad (4)$$

where  $\nu$  is true anomaly and  $\omega$  is the argument of periapsis. As shown in Fig. 1, the basis vector  $\hat{e}_r$  is a unit vector along the radial line from the center of the Earth to the tether center of mass,  $\hat{e}_w$  is normal to the orbit plane, and  $\hat{e}_\theta$  completes the triad.

Substituting Eqs. (2–4) into Eq. (1), the force induced from a current in the tether is

$$F = (LI\mu_m/r^3)[\cos i \hat{e}_\theta - \cos(\omega + \nu) \sin i \hat{e}_w] \quad (5)$$

Received 19 April 2002; revision received 28 January 2003; accepted for publication 23 April 2003. This material is declared a work of the U.S. Government and is not subject to copyright protection in the United States. Copies of this paper may be made for personal or internal use, on condition that the copier pay the \$10.00 per-copy fee to the Copyright Clearance Center, Inc., 222 Rosewood Drive, Danvers, MA 01923; include the code 0731-5090/03 \$10.00 in correspondence with the CCC.

\*Assistant Professor, Department of Aeronautics and Astronautics; Steven.Tragesser@afit.edu. Senior Member AIAA.

†Graduate Student, Department of Aeronautics and Astronautics.

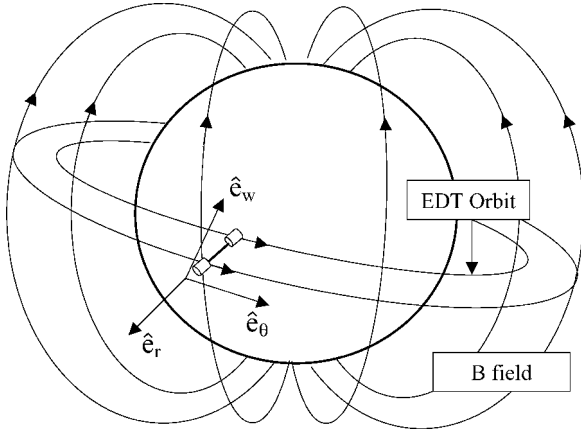


Fig. 1 Electrodynamic tether concept.

Some observations can be made immediately. There is no radial component because the force is perpendicular to the current. Also, because the force is perpendicular to the magnetic field lines, out-of-plane forces cannot be attained when the orbit is coplanar with the magnetic equator,  $i = 0$  deg, and in-plane forces cannot be attained when the orbit is polar with respect to the magnetic field,  $i = 90$  deg.

Substituting the components of the tether force into the general perturbation equations<sup>12</sup> gives the equations governing the evolution of the orbital elements for a known current:

$$\begin{aligned} \frac{da}{dt} &= \frac{2a\sqrt{1-e^2}}{nma^4} LI\mu_m \cos i \\ \frac{de}{dt} &= \frac{\sqrt{1-e^2}}{nma^2 e r^4} LI\mu_m [a^2(1-e^2) - r^2] \cos i \\ \frac{d\omega}{dt} &= \frac{\sqrt{a(1-e^2)}}{me\sqrt{\mu} r^3} LI\mu_m \sin v \cos i \left(1 + \frac{1}{1+e \cos v}\right) \\ &\quad + \frac{1}{nma^2 \sqrt{1-e^2} r^2} LI\mu_m \sin(v+\omega) \cos(v+\omega) \cos i \\ \frac{di}{dt} &= -\frac{1}{nma^2 \sqrt{1-e^2} r^2} LI\mu_m \cos^2(v+\omega) \sin i \\ \frac{d\Omega}{dt} &= -\frac{1}{nma^2 \sqrt{1-e^2} r^2} LI\mu_m \sin(v+\omega) \cos(v+\omega) \end{aligned} \quad (6)$$

where  $n$  is the mean motion and  $m$  is the total system mass.

The guidance scheme developed here does not control the phase of the orbit, for example, true anomaly. This parameter is very sensitive to errors in semimajor axis, so controlling it with the first-order equations to be developed is not reasonable. If this guidance scheme were used in actual rendezvous operations, a segment of the mission would need to be designated to match the phase.

Equations (6) become ill conditioned for eccentricities approaching zero. To investigate these cases, a different set of variables, such as the equinoctial elements, would be more suitable.<sup>13</sup>

The distance to the spacecraft is a function of the osculating elements:

$$r = \frac{a(1-e^2)}{1+e \cos v} \quad (7)$$

Substituting this equation into Eqs. (6) and expanding the expressions in terms of eccentricity yields

$$\begin{aligned} \frac{da}{dt} &= \frac{2L\mu_m \cos i}{nma^3} I [1 + 4e \cos v + \mathcal{O}(e^2)] \\ \frac{de}{dt} &= \frac{L\mu_m \cos i}{nma^4} I [2 \cos v + 5e \cos^2 v + e + \mathcal{O}(e^2)] \end{aligned}$$

$$\begin{aligned} \frac{d\omega}{dt} &= \frac{L\mu_m \cos i}{nma^4} I \left\{ \frac{2 \sin v}{e} + 5 \cos v \sin v + \cos(v+\omega) \sin(v+\omega) \right. \\ &\quad \left. + 2e \cos v [\cos v + \cos(v+\omega) \sin(v+\omega)] + \mathcal{O}(e^2) \right\} \end{aligned}$$

$$\frac{di}{dt} = -\frac{L\mu_m \sin i}{nma^4} I \cos^2(v+\omega) [1 + 2e \cos v + \mathcal{O}(e^2)]$$

$$\frac{d\Omega}{dt} = -\frac{L\mu_m}{nma^4} I \cos(v+\omega) \sin(v+\omega) [1 + 2e \cos v + \mathcal{O}(e^2)] \quad (8)$$

The higher-order terms in eccentricity will be neglected because this parameter is small for the LEO maneuvers applicable to this concept.

These equations can be integrated for a particular current to determine changes in the orbital elements. The form of the current law is determined next.

### Current Law

To achieve a desired change in the orbital elements the current in the tether is modulated as the electrodynamic tether orbits the Earth. The first task in developing the current law is to find a form that will yield secular changes in the orbital elements. This is done by analyzing the general perturbation equations in Eqs. (8) and determining the current that will yield an integral with a secular term. As a first-order approximation, the orbital elements  $a$ ,  $e$ ,  $i$ ,  $\Omega$ , and  $\omega$  on the right-hand side of Eqs. (8) will be assumed constant for the integration. Therefore, the changes in the orbital elements are given by

$$\begin{aligned} \Delta a &\approx \frac{2L\mu_m \cos i}{nma^3} \int_{t_0}^{t_f} I (1 + 4e \cos v) dt \\ \Delta e &\approx \frac{L\mu_m \cos i}{nma^4} \int_{t_0}^{t_f} I (2 \cos v + 5e \cos^2 v + e) dt \\ \Delta \omega &\approx \frac{L\mu_m \cos i}{nma^4} \int_{t_0}^{t_f} I \{ 2 \sin v / e + 5 \cos v \sin v \\ &\quad + \cos(v+\omega) \sin(v+\omega) + 2e \cos v [\cos v \\ &\quad + \cos(v+\omega) \sin(v+\omega)] \} dt \\ \Delta i &\approx -\frac{L\mu_m \sin i}{nma^4} \int_{t_0}^{t_f} I \cos^2(v+\omega) (1 + 2e \cos v) dt \\ \Delta \Omega &\approx -\frac{L\mu_m}{nma^4} \int_{t_0}^{t_f} I \cos(v+\omega) \sin(v+\omega) (1 + 2e \cos v) dt \end{aligned} \quad (9)$$

The expression for semimajor axis is the only one with a constant in the integral. Therefore, applying a positive constant current to the tether results in a change in semimajor axis that increases linearly with time. The second term in the integral will average out after each orbit and not significantly contribute to the behavior of the semimajor axis. Similarly, for the integral for eccentricity, if a current law of

$$I = \cos v \quad (10)$$

is adopted, then we have a  $\cos^2 v$  term in the integral for  $\Delta e$ . This term integrates to yield a secular change in eccentricity. Proceeding in this fashion, current laws can be found that provide a secular change in each of the orbital elements. The currents and their corresponding orbital elements are given in Table 1.

These relationships agree with those determined by Carroll<sup>14</sup> (also see Ref. 15). These references do not mention, however, that, in addition to these effects, there is some coupling between the various current laws and the orbital elements. For example, a dc current primarily affects semimajor axis, but the  $\cos^2(v+\omega)$  term in the

**Table 1** Current laws and corresponding orbital elements

Current law <sup>a</sup>	Orbital element
DC	Semimajor axis
$\cos \nu$	Eccentricity
$\sin \nu$	Argument of perigee
$\cos[2(\nu + \omega)]$	Inclination
$\sin[2(\nu + \omega)]$	Line of nodes

<sup>a</sup>Current laws provide secular change in these corresponding orbital elements.

inclination equation in Eq. (9) also produces a secular effect. This coupling is observed in Ref. 4 and will be treated in the next section.

To complete the development of the current law, a superposition principle is assumed. That is, a linear combination of the five independent laws described earlier is employed to attain any desired set of the five independent orbital elements. Thus, the final form of the current law is

$$I = X_1 + X_2 \cos \nu + X_3 \sin \nu + X_4 \cos[2(\nu + \omega)] + X_5 \sin[2(\nu + \omega)] \quad (11)$$

where the  $X_i$  are coefficients that will be calculated to maneuver the vehicle to the final desired orbit.

### Guidance Scheme

The guidance algorithm must determine the values of the  $X_i$  coefficients of the current law that produce the desired change in the orbital elements. The secular changes in the orbital elements are found by substituting the current law from Eq. (11) into Eqs. (9) and taking an averaged integral over one period of the orbit. This method eliminates the periodic effects. To perform these integrals, the independent variable is changed from time to true anomaly using the expression

$$dt = r^2/h d\nu \quad (12)$$

Expanding this expression out and neglecting terms of  $e^2$  and higher yields

$$dt = [(1 - 2e \cos \nu)/n] d\nu \quad (13)$$

Letting  $\Delta = [\Delta a \ \Delta e \ \Delta \omega \ \Delta i \ \Delta \Omega]^T$  and  $X = [X_1 \ X_2 \ X_3 \ X_4 \ X_5]^T$  and performing the necessary integrals provides a system of equations that is linear in the unknown  $X_i$ ,

$$[A]tX = \Delta \quad (14)$$

where the elements of the constant matrix  $A$  are listed in the Appendix. The equation is linear with respect to time due to averaging over an orbital period. The  $A_{ii}$  diagonal terms are the dominant terms because most of the off-diagonal terms are multiplied by eccentricity. The off-diagonal terms represent the coupling mentioned earlier between the different terms of the control law and the orbital elements.

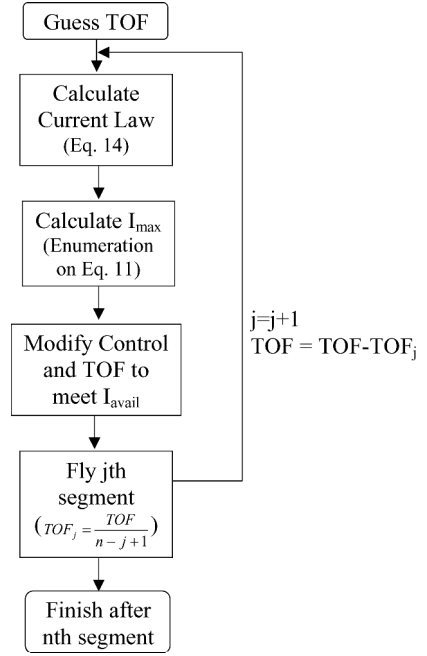
Given a desired change in orbital elements,  $\Delta$ , and the time of flight of the maneuver (TOF), Eq. (14) can be solved to determine the current law coefficients,

$$X = (1/\text{TOF})[A^{-1}]\Delta \quad (15)$$

If the duration of the maneuver is too short, however, the maximum current  $I_{\max}$  will exceed the onboard power capacity of the system,  $I_{\text{avail}}$ . To rectify this problem, the duration of the maneuver is altered to enforce the constraint on the maximum current. Because the change in orbital elements is linearly dependent on the TOF, the current can be scaled down by a constant factor and the TOF scaled up by the inverse of that same factor with the final orbit remaining unchanged (to first order). Thus, when

$$X_{\text{new}} = X_{\text{old}}(I_{\text{avail}}/I_{\max}), \quad \text{TOF}_{\text{new}} = \text{TOF}_{\text{old}}(I_{\max}/I_{\text{avail}}) \quad (16)$$

the current constraint is enforced while satisfying Eq. (15), that is, obtaining the same change in the orbital elements.

**Fig. 2** Guidance scheme.

There are three options for computing  $I_{\max}$ . A numerical simulation would provide a precise answer, but it is computationally cumbersome. Analytical derivatives of the current expression with respect to true anomaly and argument of periapsis can be set to zero and solved, but this leads to a nonlinear system of equations that must be solved numerically, which is not sufficiently robust for the intent of this study. Therefore, a crude method is used in which the current is enumerated for a 360-deg range of true anomaly and a range of argument of periapsis from  $\omega$  to  $\omega + \Delta\omega$ .

The available current  $I_{\text{avail}}$  is assumed to be a constant dependent on the spacecraft. This quantity is the maximum current that is being forced through the tether by the spacecraft (as opposed to the emf resulting from the spacecraft motion), and so it is primarily a function of the onboard power system. However, in reality, this value will vary depending on a number of factors that are not considered here, such as the plasma density and duty scheduling of the spacecraft.

For maneuvers with a large change in the orbital elements, the first-order assumption that the orbital elements are constant for the integration of Eqs. (8) is not valid. Unfortunately, very accurate solutions of these integrals would need to be numerical, which would then make it impossible to develop analytic expressions to calculate the coefficients of the current law. Because the aim of this work is to produce a computationally efficient and robust design for concept exploration, a simpler approach is taken. To improve the accuracy of the guidance scheme, the maneuver can be broken into several segments. By the recalculation of the current law several times during the maneuver, the guidance scheme has an opportunity to correct for the errors introduced by the inexact integrals. The guidance scheme employed is summarized in Fig. 2.

### Results

A numerical simulation is used to validate the guidance scheme for arbitrary orbit maneuvers in LEO. The equation of motion for the electrodynamic tether system is

$$\ddot{\mathbf{r}} = -(\mu/r^3)\mathbf{r} + (1/m)\mathbf{F} \quad (17)$$

where  $\mathbf{r}$  is the position of the spacecraft system center of mass with respect to the center of the Earth,  $\mathbf{F}$  is the perturbing force due to the electrostatics [Eq. (5)], and  $m$  is the total system mass. The corresponding scalar equations of motion are integrated using a Runge-Kutta 5/6 variable step integration with a tolerance of  $1 \times 10^{-10}$ .

For the examples to follow, the mass of the electrodynamic tethered vehicle is 1000 kg, with a maximum current of 5 A and a tether length of 15 km (Ref. 2).

### Orbit Raising

The first example demonstrates an increase in the semimajor axis of a LEO satellite at an inclination of 30 deg with respect to the geomagnetic equator. The orbit is nearly circular with an eccentricity of 0.02, a semimajor axis of 6878 km, and an argument of perigee of 30 deg. The results are invariant with respect to the initial longitude of the ascending node. The desired changes in the orbital elements are

$$\Delta a = 200 \text{ km}, \quad \Delta e = \Delta \omega = \Delta i = \Delta \Omega = 0 \quad (18)$$

To achieve this maneuver, the current law and TOF are

$$I = 1.65 - 0.04 \cos \nu - 0.02 \sin \nu - 3.31 \cos[2(\nu + \omega)] \\ + 0 \sin[2(\nu + \omega)]$$

$$\text{TOF} = 58 \text{ h } 10 \text{ min} \quad (19)$$

As expected, the dc current is significant to induce a change in orbit energy. However, the dc current also causes a significant change in inclination because the  $A_{41}$  term of Eq. (14) is large. To keep the inclination constant, the  $\cos[2(\nu + \omega)]$  term must, therefore, also be large, as shown in Eq. (19). The other two nonzero terms are needed to offset small off-diagonal terms of the  $A$  matrix.

Performing the simulation for this current law leads to the results shown in Figs. 3–5. The semimajor axis exhibits the desired linear increase, whereas the other variables exhibit negligible secular behavior. The current shows the 1.65 A dc offset with a 3.3-A sinusoidal oscillation. The period of the oscillation is approximately half the orbital period, so that this oscillation cycles through many oscillations in Fig. 4. A closeup of the first two orbits is shown in Fig. 5. These plots illustrate the potential difficulty in numerically optimizing the trajectory for electrodynamic maneuvers. To capture the rapidly changing control, many parameter optimization techniques would require thousands of degrees of freedom to capture the salient behavior.

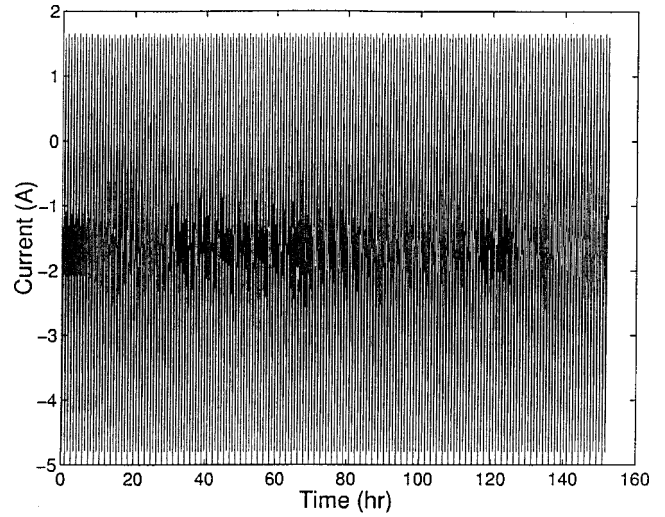


Fig. 4 Tether current to raise orbit.

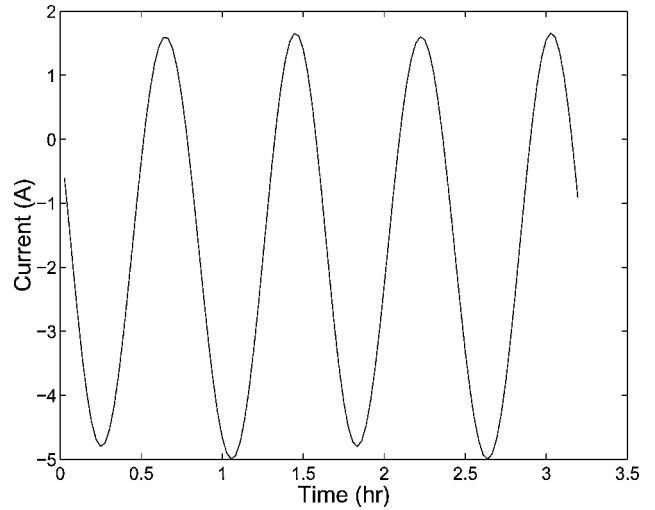


Fig. 5 Closeup of Fig. 4.

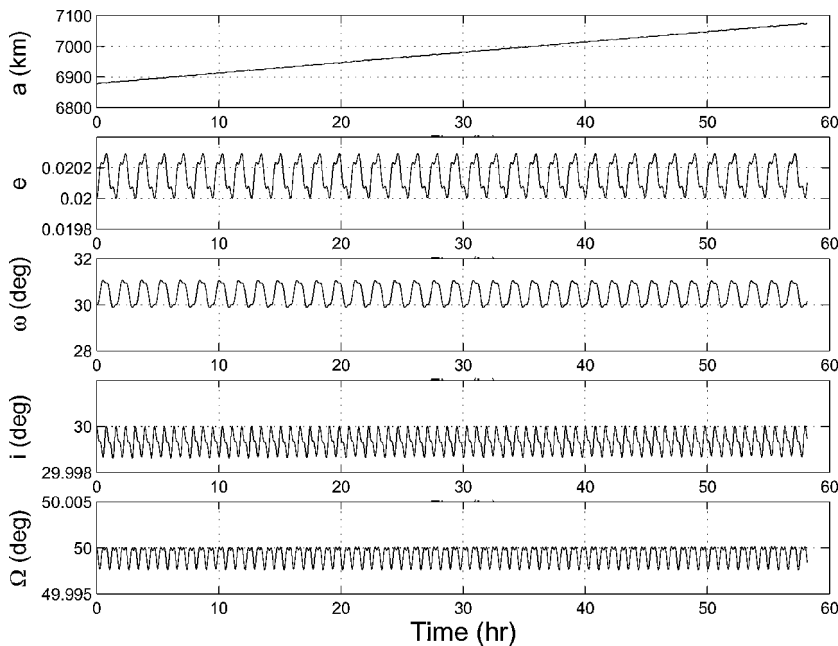


Fig. 3 Orbit raising example.

The error in the final orbital elements for the orbit raising is

$$\begin{aligned}\Delta a_{\text{err}} &= -3.88 \text{ km}, & \Delta e_{\text{err}} &= 0.0001, & \Delta \omega_{\text{err}} &= 0.13 \text{ deg} \\ \Delta i_{\text{err}} &= -0.0005 \text{ deg}, & \Delta \Omega_{\text{err}} &= -0.002 \text{ deg}\end{aligned}\quad (20)$$

These errors have two sources. The first is the periodic nature of the disturbances. For this example, the short-period amplitudes of the five variables in Fig. 3 are 1 km, 0.0002, 0.5 deg, 0.001 deg, and 0.001 deg, respectively. Because the guidance equations only account for the secular behavior, errors below these amplitudes cannot be entirely eliminated. The second error source is the assumption that the orbital elements on the right-hand side of Eqs. (8) are constant. As the electrodynamic tether force changes the orbit, the secular change that a given law produces [according to Eq. (14)] will change. For the preceding example, the slope of the semimajor axis at the start of the maneuver is 3.4 km/h, whereas the slope at the end of the maneuver is 3.3 km/h. Because the maneuver time is based on the initial secular rates of change of the variables, errors are introduced. In this example, the semimajor axis falls short of the target because the rate of change drops as the semimajor axis increases.

This second error source can be reduced if the guidance is employed in several phases, as shown in Fig. 2. Each phase has a new guidance law that is calculated based on an updated set of orbital elements. The same orbit raising maneuver was simulated with five separate calculations of the current law spaced out roughly 12 h apart during the maneuver. The plots of the semimajor axis and current are similar to Figs. 3 and 4, but the final errors are improved:

$$\begin{aligned}\Delta a_{\text{err}} &= -0.24 \text{ km}, & \Delta e_{\text{err}} &= 0, & \Delta \omega_{\text{err}} &= 0.05 \text{ deg} \\ \Delta i_{\text{err}} &= 0.0005 \text{ deg}, & \Delta \Omega_{\text{err}} &= -0.0004 \text{ deg}\end{aligned}\quad (21)$$

Although the errors are much smaller, they do not asymptotically approach zero as the number of guidance corrections gets large. The inaccuracy results from neglecting the periodic effects in the orbital elements.

#### Inclination Change

The next scenario demonstrates a decrease in the orbital inclination for the same LEO satellite considered in the earlier example.

The desired changes in the orbital elements are

$$\Delta i = -5 \text{ deg}, \quad \Delta a = \Delta e = \Delta \omega = \Delta \Omega = 0 \quad (22)$$

The current law and TOF are

$$\begin{aligned}I &= 0 - 0.01 \cos \nu + 0.02 \sin \nu + 4.98 \cos[2(\nu + \omega)] \\ &\quad + 0 \sin[2(\nu + \omega)]\end{aligned}$$

$$\text{TOF} = 803 \text{ h } 32 \text{ min} \quad (23)$$

The maneuver duration is quite long because the electromagnetic tether can only generate forces perpendicular to the Earth's magnetic field lines. Therefore, for this case, the component of the electromagnetic force perpendicular to the orbit plane is relatively small. As a general principle, changes in the orbit inclination and line of nodes can be most effectively performed at higher inclinations; changes in orbital energy and eccentricity are most effective at lower inclinations.

The errors in the final orbital elements for the inclination change are significant for semimajor axis and inclination; the periapsis error is small compared to its periodic amplitude:

$$\begin{aligned}\Delta a_{\text{err}} &= -0.77 \text{ km}, & \Delta e_{\text{err}} &= -0.0003, & \Delta \omega_{\text{err}} &= 0.11 \text{ deg} \\ \Delta i_{\text{err}} &= 0.36 \text{ deg}, & \Delta \Omega_{\text{err}} &= 0.002 \text{ deg}\end{aligned}\quad (24)$$

The case was also simulated for five corrections in the guidance law over the duration of the maneuver. The final orbit is closer to the desired state (particularly in the variable that is being changed, inclination):

$$\begin{aligned}\Delta a_{\text{err}} &= 0.54 \text{ km}, & \Delta e_{\text{err}} &= 0, & \Delta \omega_{\text{err}} &= -0.16 \text{ deg} \\ \Delta i_{\text{err}} &= 0.02 \text{ deg}, & \Delta \Omega_{\text{err}} &= 0.0003 \text{ deg}\end{aligned}\quad (25)$$

The orbital elements for this simulation are plotted in Fig. 6.

#### General Orbit Change

The electrodynamic tether achieves a simultaneous change in all of the orbital elements for this final example, validating the superposition rule assumed in Eq. (11). The electrodynamic tether is

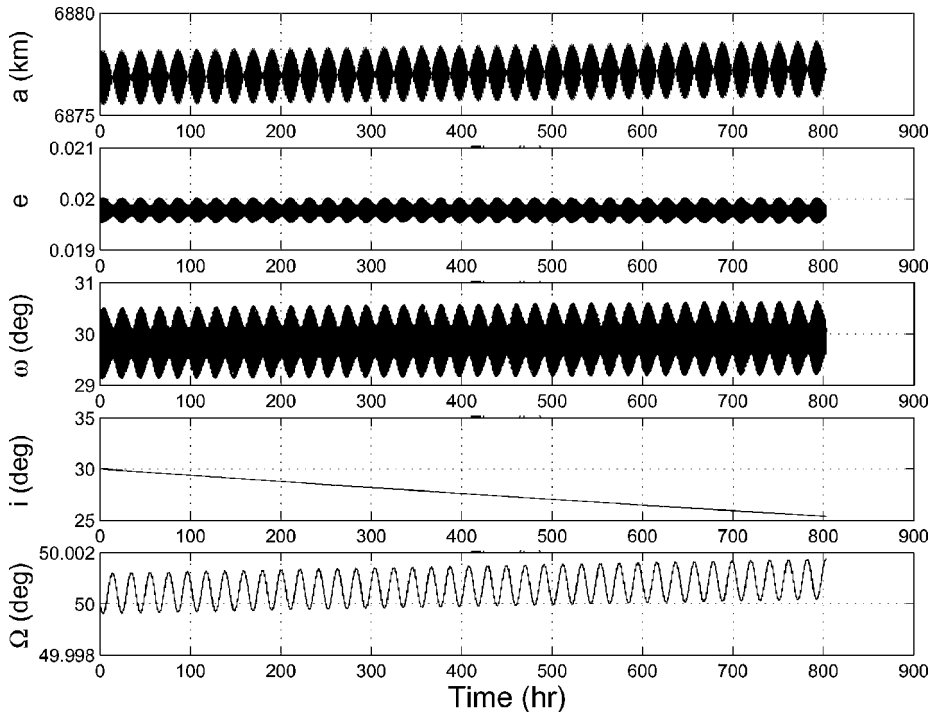


Fig. 6 Inclination change example.

initially coorbital with the Landsat-4 satellite and will transfer to the Landsat-5 satellite. (Suppose, for example, that both had a flawed sensor that needed to be replaced.) The initial orbit is<sup>‡</sup>

$$\begin{aligned} a_0 &= 6961 \text{ km}, & e_0 &= 0.001, & \omega_0 &= 4.7 \text{ deg} \\ i_0 &= 98.2 \text{ deg}, & \Omega_0 &= 90.4 \text{ deg} \end{aligned} \quad (26)$$

To rendezvous with Landsat-5, the electrodynamic tether system must perform the following orbital maneuvers:

$$\begin{aligned} \Delta a &= 120 \text{ km}, & \Delta e &= -0.0001, & \Delta \omega &= 29.3 \text{ deg} \\ \Delta i &= -0.06 \text{ deg}, & \Delta \Omega &= -8.9 \text{ deg} \end{aligned} \quad (27)$$

To effect these changes simultaneously, current law and TOF are

$$\begin{aligned} I &= -0.43 + 0 \cos \nu - 0.03 \sin \nu + 0.90 \cos[2(\nu + \omega)] \\ &\quad + 4.45 \sin[2(\nu + \omega)] \end{aligned}$$

$$\text{TOF} = 825 \text{ h } 2 \text{ min} \quad (28)$$

The largest term in the current law is the  $\sin[2(\nu + \omega)]$  component, which is responsible for the change in the line of nodes. This plane change is large, resulting in a long TOF.

A simulation with five segments in the guidance scheme successfully achieves the desired orbit with the following errors for the final elements:

$$\begin{aligned} \Delta a_{\text{err}} &= 0.28 \text{ km}, & \Delta e_{\text{err}} &= 0, & \Delta \omega_{\text{err}} &= 1.2 \text{ deg} \\ \Delta i_{\text{err}} &= -0.002 \text{ deg}, & \Delta \Omega_{\text{err}} &= -0.003 \text{ deg} \end{aligned} \quad (29)$$

### Conclusions

The developed guidance algorithm is capable of performing any LEO transfer given a sufficiently long maneuver time. The trajectories generated by this guidance scheme are not optimal. The goal for this study was to keep the calculations simple and computationally reasonable to implement in an onboard system or to generate rapidly many trajectories for concept exploration. There is no iterative calculation requiring convergence or numerical simulation in the guidance equations. However, the guidance scheme can be split into multiple segments to improve its accuracy in reaching the final orbit.

### Appendix: Elements of Constant Matrix A

$$\begin{aligned} A_{11} &= 8Ca \cos i, & A_{12} &= 8Cae \cos i \\ A_{13} &= 0, & A_{14} &= 0, & A_{15} &= 0 \\ A_{21} &= 6Ce \cos i, & A_{22} &= 4C \cos i, & A_{23} &= 0 \\ A_{24} &= Ce \cos i \cos(2\omega), & A_{25} &= Ce \cos i \sin(2\omega) \\ A_{31} &= 4Ce \cos i, & A_{32} &= 0, & A_{33} &= 4C \cos i/e \end{aligned}$$

$$A_{34} = -C \cos i \sin(2\omega), \quad A_{35} = C \cos i [\cos(2\omega) + 1]$$

$$A_{41} = -2C \sin i, \quad A_{42} = 0, \quad A_{43} = 0$$

$$A_{44} = -C \sin i, \quad A_{45} = 0$$

$$A_{51} = 0, \quad A_{52} = 0, \quad A_{53} = 0$$

$$A_{54} = 0, \quad A_{55} = -C$$

where the constant  $C$  is

$$C = \frac{L\mu_m}{4mna^4}$$

### References

- <sup>1</sup>Gilchrist, B., Jensen, K., Severns, J., and Gallimore, A., "Field Emitter Array Cathodes (FEACs) for Space Applications," *Proceedings of the NASA/JPL/MSFC/AIAA 10th Annual Advanced Space Propulsion Workshop*, Jet Propulsion Lab., Pasadena, CA, 1999, pp. 609–622.
- <sup>2</sup>Vas, I. E., Kelly, T. J., and Scarl, E. A., "Space Station Reboost with Electrodynamic Tethers," *Journal of Spacecraft and Rockets*, Vol. 37, No. 2, 2000, pp. 154–164.
- <sup>3</sup>Hoyt, R., and Forward, R., "Performance of the Terminator Tether for Autonomous Deorbit of LEO Spacecraft," *Journal of the Astronautical Sciences*, Vol. 37, No. 4, 1989, pp. 433–450.
- <sup>4</sup>West, B., and Gilchrist, B., "Life Extension and Orbit Maneuvering Strategies for Small Satellites in Low Earth Orbit Using Electrodynamic Tethers," AIAA Paper 2001-1139, Jan. 2001.
- <sup>5</sup>Peláez, J., López-Rebollal, L. M., and Ahedo, E., "Dynamic Stability of a Bare Tether as a Deorbiting Device," American Astronautical Society, AAS Paper 02-200, Jan. 2002.
- <sup>6</sup>Lorenzini, E. C., "In-Space Transportation with Tethers," NASA Rept. 19990100963, 1999.
- <sup>7</sup>Santangelo, A., Johnson, L., Gilchrist, B., Hoffman, J., Hoffman, J., Lorenzini, E., and Estes, R., "Advancing Electrodynamic Tethers to Commercially Viable Systems—STEP-AIRSEDS," *Proceedings of the NASA/JPL/MSFC/AIAA 10th Annual Advanced Space Propulsion Workshop*, Vol. 2, Jet Propulsion Lab., Pasadena, CA, 1999, pp. 602–622.
- <sup>8</sup>Gilchrist, B. E., Johnson, L., and Bilen, S. G., "Space Electrodynamic Tether Propulsion Technology: System Considerations and Future Plans," AIAA Paper 99-2841, June 1999.
- <sup>9</sup>Yamagiwa, Y., "Performance Analysis of Electrodynamic Tether Orbit Transfer System for Round Trip Mission," *Journal of Space Technology and Science*, Vol. 13, No. 1, 1997, pp. 17–25.
- <sup>10</sup>Beletsky, V. V., and Levin, E. M., *Dynamics of Space Tether Systems*, American Astronautical Society, San Diego, CA, 1993.
- <sup>11</sup>Peláez, J., López-Rebollal, R. M., and Lorenzini, E. C., "Damping in Rigid Electrodynamic Tethers on Inclined Orbits," American Astronautical Society, AAS Paper 01-190, Feb. 2001.
- <sup>12</sup>Chobotov, V. A., Ed., *Orbital Mechanics*, 2nd ed., AIAA, Reston, VA, 1996, p. 200.
- <sup>13</sup>Vallado, D. A., *Fundamentals of Astrodynamics and Applications*, McGraw-Hill, New York, 1997, pp. 142, 143.
- <sup>14</sup>Carroll, J. A., *Guidebook for Analysis of Tether Application*, Martin Marietta Corp., Contract RH4394049, Raleigh, NC, March 1985.
- <sup>15</sup>Cosmo, M. L., and Lorenzini, E. C., *Tethers in Space Handbook*, 3rd. ed., NASA Marshall Space Flight Center Grant NAG8-1160, 1997, pp. 182–185.

<sup>‡</sup>Data available online from Kelso, T. S., "Celestrak," at <http://www.celestrak.com/> [cited 7 August 2003].